Transformations in the medium-range order of fused silica under high pressure

Lílian P. Dávila,[1,2,*] Maria-José Caturla,[2,3] Alison Kubota,[2] Babak Sadigh,[2] Tomás Díaz de la Rubia,[2] James F. Shackelford,[1] Subhash H. Risbud,[1] and Stephen H. Garofalini [4]

[1] *Dept. of Chemical Engineering and Materials Science, University of California Davis, Davis, CA 95616*
[2] *Lawrence Livermore National Laboratory, Livermore, CA 94550*
[3] *Dept. Fisica Aplicada, Universidad de Alicante, Alicante, Spain, E-03690*
[4] *Department of Ceramic and Materials Engineering, Rutgers University, Piscataway, NJ 08854*

(Dated: September 23, 2003)

Molecular dynamics simulations of fused silica at shock pressures reproduce the experimental equation of state of this material and explain its characteristic shape. We demonstrate that shock waves modify the medium-range order of this amorphous system, producing changes that are only clearly revealed by its ring size distribution. The ring size distribution remains practically unchanged during elastic compression but varies continuously after the transition to the plastic regime.

PACS numbers: 61.43.-j, 64.30.+t, 02.70.Ns, 78.55.Qr

High-pressure experiments reveal an unusual equation of state (EOS) of amorphous silica, displaying an initial increase in compressibility with pressure and irreversible densification [1-2]. Shock loading and neutron irradiation [3-5] can also result in higher density silica glass. Under hydrostatic loads at ambient temperatures, the compaction begins at 8-10 GPa, below which the compression remains elastic [6-7]. Samples recovered from shock compressions at 10-16 GPa show evidence of permanent densification and a transition to a high-density form at about 16 GPa [8]. Experimental studies have revealed large (20-30%) permanent densifications under high pressures [9-10].

[*] Electronic address: lpdavila@ucdavis.edu

The densification of amorphous silica has been studied by many groups over several decades [2-3, 11-12]. However, only in the 1990s was it suggested that the high-density forms are unique in their structure [7,13]. Structural changes were revealed by *in situ* vibrational spectroscopy measurements [14-16] and X-ray diffraction [17]. The increase in density was attributed to the rotation of the silica tetrahedra. X-ray [18] and neutron [9] diffraction, infrared and Raman spectroscopy revealed a decrease in the average Si-O-Si angle and a small increase in the Si-O bond distance [13]. Moreover, X-ray diffraction measurements [17] have shown that the characteristic first sharp diffraction peak (FSDP) associated with the medium-range order (MRO) of these materials is significantly reduced upon densification. The structural origin of the MRO and the dynamic behavior of silica glass at high pressures have been studied extensively using molecular dynamics (MD) simulations [9, 19-22] but a completely satisfactory understanding has not yet been achieved. Recent papers have shown how the medium-range order can be manipulated experimentally [23-24], resulting in materials of scientific and technological interest, motivating further understanding of the features that determine this ordering.

We have used MD simulations with empirical potentials to study the behavior of fused silica under high pressure. The initial amorphous structure was generated using the interatomic potential reported in Webb and Garofalini [25].

We present two different simulation schemes for studying the structural transformations in fused silica under high pressures, and show that they give similar P-V relationships. In one case, a shock wave is generated in a slab containing 240,000 atoms (two free surfaces and periodic boundary conditions in the lateral directions) at 300 K, through a piston, consisting of a few designated atoms at one

end of the cell set to a constant velocity. This method (noted as M^{I}) was previously applied to the study of shock propagation in crystalline materials [26]. The shock simulation is performed typically until the shock wave reaches the free surface at the other end of the simulation box. With this method the propagation of the shock wave can be followed and its velocity measured. The results can therefore be directly compared to flyer plate experiments.

The second simulation scheme (or M^{II}) involves small periodic supercells containing 1,536 atoms at 300 K, that are compressed by reducing the volume of the supercell and allow for relaxations. The temperature in these simulations was kept constant at 300 K. A comparable method has been applied to study compression in vitreous silica [21] using minimization techniques.

The initial fused silica structure was obtained through a MD melt-quench technique similarly used in previous studies [25,27]. Periodic cells in the cubic β-cristobalite structure were melted at 7000 K for 25 ps (with a MD time step of 0.5 fs). Thereafter, they were quenched down to room temperature by a series of steps. Our starting configuration has a density of 2.205 g/cc, that is, equivalent to the experimental value for fused silica.

Using these starting configurations we applied methods I and II described above to compute the pressure-volume relationship. In the case of M^{I}, different initial velocities of the piston were used to obtain different shock velocities. The final volume and pressure was then calculated after the shock reached the back surface. For the M^{II} simulations, the volume was reduced sequentially in decrements of 2% and pressure was calculated upon reaching equilibrium, typically after 50 ps. Subsequent compression simulations were performed down to 0.58 V/V_o, where V_o is the starting volume.

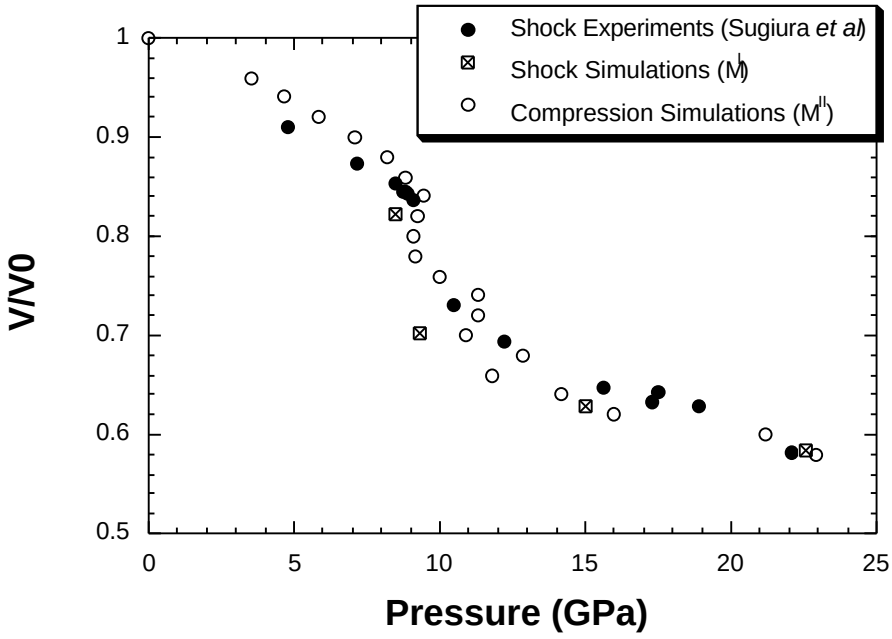

FIG. 1. Pressure-volume behavior calculated from MD simulations compared to experiments [4].

Figure 1 depicts the resulting EOS curve in the form of pressure versus relative volume, V/V_o. This figure shows the experimental results (filled circles) obtained by Sugiura *et al*. [4] using flyer plate experiments, the results from shock simulations (crossed squares) and the results from continuous compression calculations (open circles). The agreement between these MD simulations and the shock experiments is remarkable, particularly considering that the interatomic potential used was fitted only to ambient pressure and temperature conditions. It is also interesting to note the similar results between the two different types of calculations, revealing the slow dynamics and large relaxation times associated to this system. The high strain rates of our compression simulations imply that the conditions are closer to those found in shock experiments than in quasi-static experiments [6-7].

We can clearly identify two regions in the EOS curve in Fig. 1 associated with 1) linear compressions up to 0.82 V/V_o or elastic behavior and 2) asymmetric compressions starting from 0.82 V/V_o or plastic response. It is important to point out

that irreversible compaction of the glass is found in the range 9-10 GPa [6-7]. The plastic region occurs in the regime between 10-23 GPa, as shown in Fig. 1, which falls in the range of pressures known as "transformation region" [6]. We find that our simulations can accurately predict the densification of fused silica at various shock pressures. For the pressure ranges studied here values of compression up to 42% are reached during shock loading. This densification however is not permanent. We have performed relaxation of the dynamically loaded structure for the highest densification (42%). Upon relaxation the lattice expands to a final permanent densification of 20% in agreement with experiments [4-5,10].

In order to understand the structural changes occurring as the pressure increases, and to correlate them with the calculated EOS, we have performed a detailed analysis of the structure factor, the pair distribution function, the ring size distribution and the bond angle distribution of the system. In particular, the structure factor can be measured experimentally through X-ray or neutron diffraction and can provide important information about the medium-range order of amorphous materials.

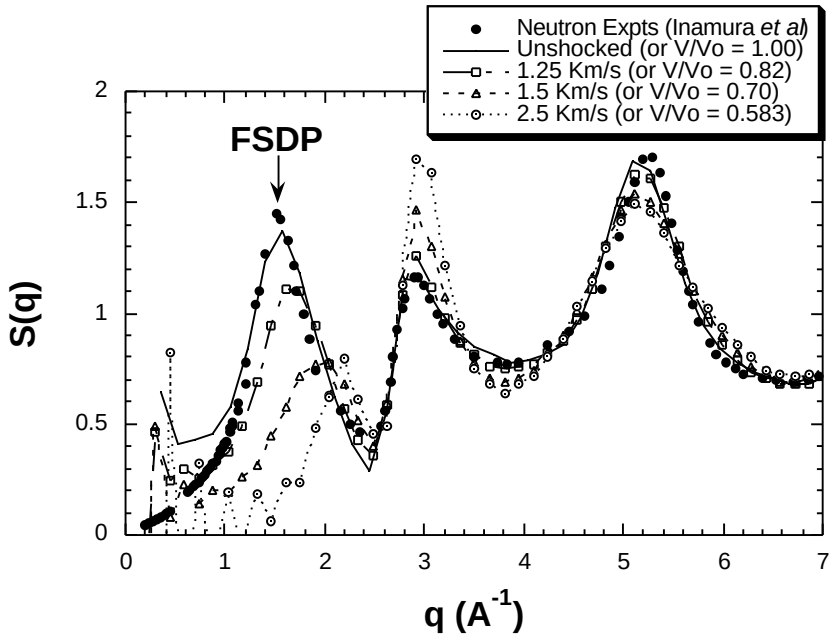

FIG. 2. Structure factor from M^I calculations. Experimental results for zero pressure are also included for comparison.

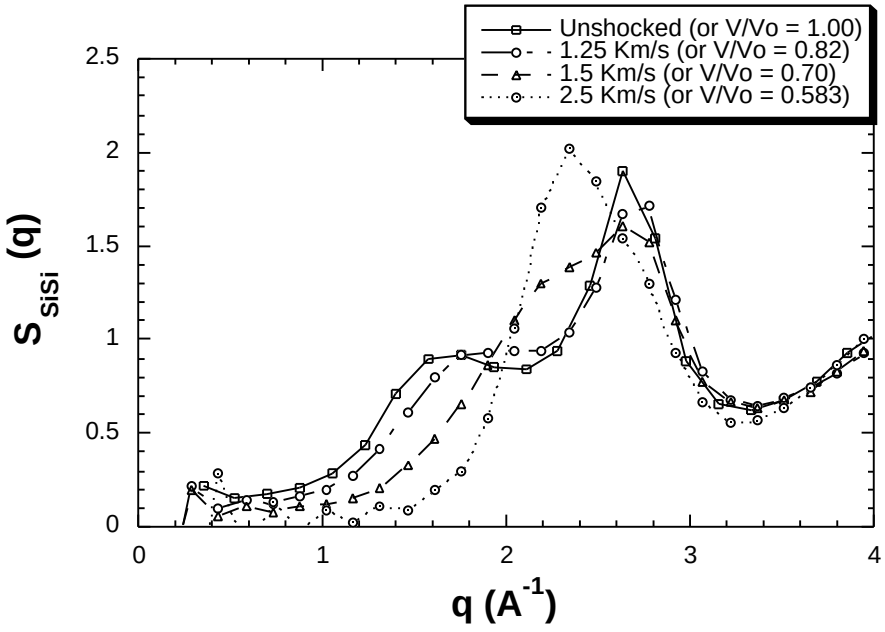

FIG.3. Partial structure factor for Si-Si from shock simulations (M^I).

One of the interesting features of silica glass is the presence of a characteristic FSDP as reported in experiments [9,17,28]. Figure 2 shows the structure factor for different pressures calculated from our M^{I} calculations. Similar results are obtained from M^{II}. In the same figure we include the experimentally measured S(q) at 0 pressure obtained by Inamura *et al.* [28] for comparison. Although there is experimentally available data for the S(q) of silica at higher pressures, these have been obtained after recovery of the sample or from diamond anvil cell experiments [9,28]. Therefore direct comparison with the simulations presented here would not be appropriate. The FSDP position occurs in the range 1-2 $Å^{-1}$ and, as observed experimentally [9,17,28], it decreases in intensity and shifts towards larger q values as the pressure increases. Figure 2 also denotes that short-range order prevails with increasing pressure in this glass as noted by the third peak in the structure factor calculations up to about 23 GPa as seen in Fig. 1. The origin of this FSDP is still controversial and many different models have been proposed, such as the one by Elliott [29] based on an interstitial-void ordering. In our simulations we observe a continuous decrease in the intensity of the FSDP with pressure, however no significant changes are observed at the point of transition between elastic and plastic behavior. The same behavior is observed in the pair correlation function. Although changes in the height and width of the peaks are observed with pressure, comparable to previous studies [9,22], none of these changes reveal clearly the transition between elastic and plastic regimes, as seen in the EOS.

The total structure factor shown in Figure 2 is a linear combination of the Si-Si, Si-O, and O-O partial structure factors (PSF). It is thus instructive to study the evolution of these PSF with pressure. We find that the Si-O and O-O short-range order is only slightly changed with pressure, however the pre-peak in both cases follow the same trend as in the total structure factor, i.e. moving out to larger q-

values with diminishing intensity. A more interesting and unique behavior is observed in the Si-Si PSF, where the pre-peak and the first peak are merged together and eventually only one peak is observed, as shown in Figure 3 for the case of M^{I}. The origin of this behavior can be traced to changing Si-Si short-range order with pressure. The real-space Si-Si pair-correlation function reveals that the average nearest-neighbor distance between Si atoms decreases with pressure, in agreement with previous calculations [9,18,29], while the corresponding first peak in the Si-Si pair-correlation function reduces in magnitude and broadens significantly into a structure with almost double-peak character. From this analysis, however, we still can not extract a clear correlation between the changes in the structure factor and the EOS.

Most interesting are those changes revealed by the ring size distribution, which characterizes the medium-range order of these amorphous materials. Rings are defined as the shortest closed loop of Si-O bonds. Fused silica consists of a distribution centered on six-member rings. Figure 4 shows the number of rings (normalized to their value at zero pressure) as a function of densification for the two types of simulations presented here. Note the ring evolution (a) for M^{I} and (b) for M^{II} and for different sizes of rings. The ring distribution was calculated using the "shortest-path" criterion [26], assuming that stable bonds are formed at distances smaller than 2 Å.

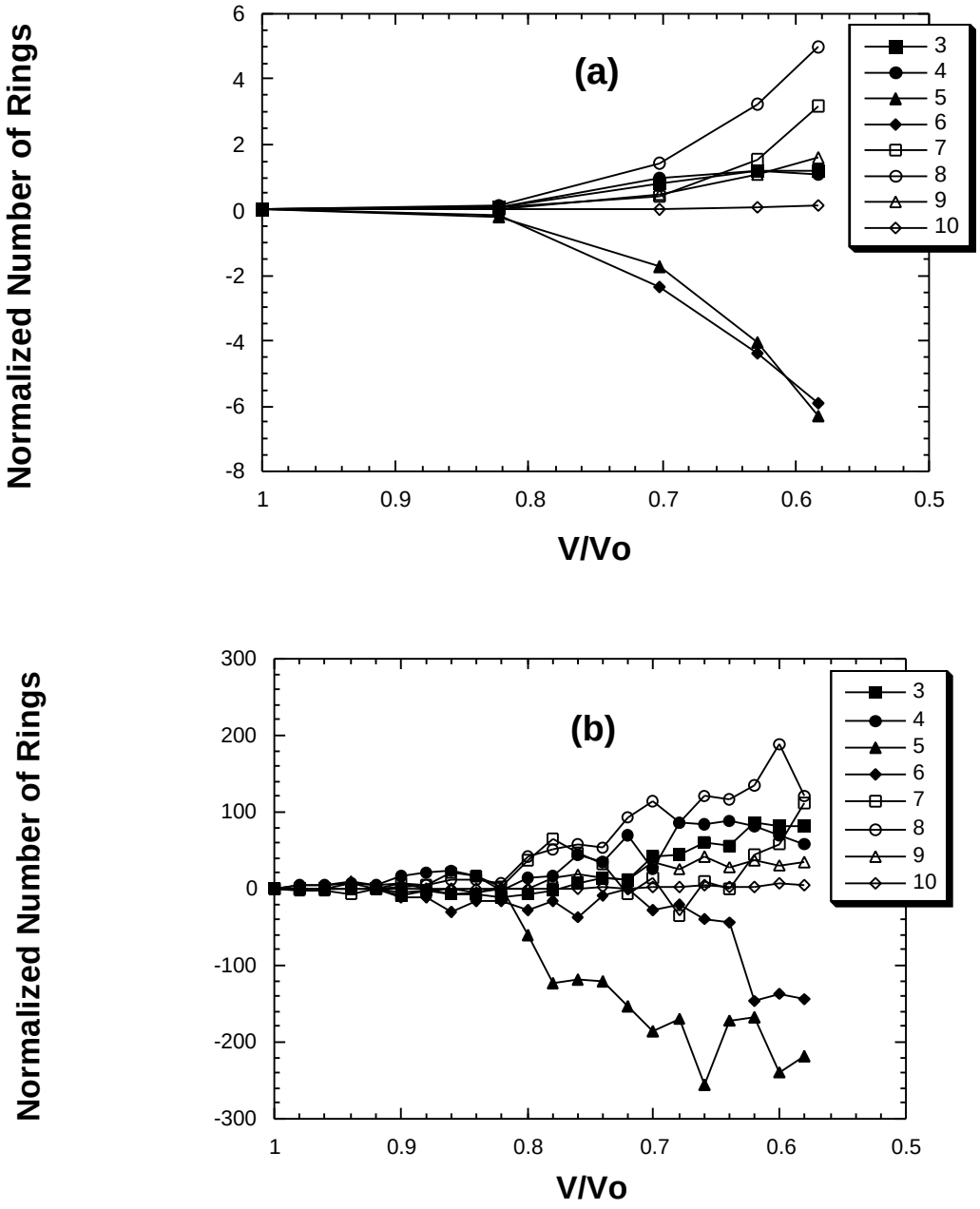

FIG.4. Normalized number of rings as a function of volume in (a) shock simulations (M^{I}) and (b) continuous compression simulations (M^{II}).

These simulations show that the ring size distribution does not change from 1 to 0.82 V/V_o, consistent with the linearity of the EOS curve in this same region. Therefore, in this regime, no structural changes are occurring, and the compression is elastic. Above 18% compression, large changes in the ring distributions in both simulations are observed. These changes correlate well with the EOS curve between 0.82 and 0.64 V/V_o. There is a continuous decrease in the number of rings of size 5 and 6 during the plastic regime and an increase in the number of both smaller and larger rings. Qualitatively both simulations show the same behavior. However, dynamic simulations show a decrease in rings of size 6 at lower pressures than for the case of continuous compression. This discrepancy could be due to size and temperature differences between the two simulations. The temperatures reached in method M^I are higher than in M^{II}. This effect would be particularly noticeable at the highest pressures, but would not change qualitatively the trends in the EOS. Although significant changes in the structure are observed during increasing pressure, the average ring size for silica glass is still 6, since it preserves the tetrahedral structure.

Figures 4 (a and b) also show that the smaller (3- and 4-member) rings increase in total number upon compression in the region between 0.82 and 0.64 V/V_o. These small rings are very close to planar rings and present vibration frequencies that can be detected by Raman spectroscopy. Raman measurements of compressed silica glass have shown enhancement of the D_1 and D_2 lines associated to rings of size 4 and 3 respectively [15], in agreement with the results of our model. Moreover, the number of rings of size 3 and 4 increases with pressure up to about 0.625 V/V_o at which point it saturates for the case of rings of size 3, while the number of 4-member rings seems to decrease. Recent experiments by Krol *et al.* have shown similar behavior in the Raman spectra of laser irradiated silica glasses [16].

The bond angle distribution of both O-Si-O and Si-O-Si also change continuously with pressure, even in the elastic regime. This implies that although the distribution and number of rings is not changing in the elastic regime, their geometry must be changing, as expected. The O-Si-O bond angle distribution broadens with pressure while keeping a value centered around 109° to 108° for the highest pressures. The Si-O-Si bond angle distribution shifts towards lower values as pressure increases, in agreement with experimental observations [17]. At the highest pressures this distribution presents two broad peaks, as shown earlier in simulations by Vashishta *et al.* [20]. It is interesting to note that this change from a single peak to a double peak seems to occur in the elastic to plastic regime, although it is hard to identify clearly the point of transition.

The above analysis shows that the behavior of the EOS can be explained by the changes observed in the ring size distribution and that these changes are not clearly reflected in other characteristic parameters, such as the intensity of the FSDP or its width. Both of them decrease continuously with pressure even during the elastic regime, where we find no variations in the ring size distribution. Therefore, the origin of this peak cannot be related only to the total number of rings present or its distribution.

In summary, we have investigated the behavior of an amorphous system, fused silica, under pressure using atomistic simulations. Our MD simulations of both dynamic shock loading and continuous compression at constant temperature reproduce the equation of state of flyer plate experiments. The transition between elastic and plastic behavior is correlated to changes in the ring size distribution of this amorphous system, and is not clearly reflected by other parameters such as pair correlation function, structure factor or bond angle distributions. Therefore, these

changes must be governed by the preserved connectivity of these network structures revealed by a decrease in 5- and 6-member rings at high pressure that compensates with an increase of both smaller and larger rings.

Acknowledgements

This work was performed under the auspices of the U. S. Department of Energy, Lawrence Livermore National Laboratory under Contract No. W-7405-Eng-48. Funding was provided by the Department of Energy Office of Basic Energy Sciences. One of the authors (MJC) wants to thank the Spanish MCYT for support through the Ramon y Cajal program. Thanks to E. Bringa for useful discussions.

References

[1]P. W. Bridgman and I. Simon, J. Appl. Phys. **24**, 405 (1953).
[2]R. Roy and H. M. Cohen, Nature (London) **190**, 798 (1961).
[3]W. Primak, *Compacted States of Vitreous Silica-Studies of Radiation Effects in Solids* (Gordon and Breach, New York, 1975).
[4]H. Sugiura, K. Kondo, and A. Sawaoka, J. Appl. Phys. **52**, 3375 (1981).
[5]H. Sugiura, R. Ikeda, K. Kondo, and T. Yamadaya, J. Appl. Phys. **81**, 1651 (1997).
[6]C. S. Zha, R. J. Hemley, H. K. Mao, T. S. Duffy, and C. Meade, Phys. Rev. B **50**, 13105 (1994).
[7]A. Polian and M. Grimsditch, Phys. Rev. B **41**, 6086 (1990).
[8]J. Wackerle, J. Appl. Phys. **33**, 922 (1962).
[9]S. Susman, K. J. Volin, D. L. Price, M. Grimsditch, J. P. Rino, R. K. Kalia, P. Vashishta, G. Gwanmesia, Y. Wang, and R. C. Liebermann, Phys. Rev. B **43**, 1194 (1991).
[10]J. Wong, D. Haupt, J. H. Kinney, J. Ferreira, I. Hutcheon, S. Demos, and M. R. Kozlowski, *Proc. SPIE* **4347**, 466 (2001).
[11]R. Bruckner, J. Non-Cryst. Solids **5**, 123 (1970).
[12]A. G. Revesz, J. Non-Cryst. Solids **7**, 77 (1972).
[13]R. J. Hemley, C. T. Prewitt, and K. J. Kingma, *Reviews in Mineralogy, Silica: Physical Behavior, Geochemistry, and Materials Applications* (Mineralogical Society of America, Washington D.C., 1994), Vol. 29, Chap. 2.
[14]Q. Williams and R. Jeanloz, Science **239**, 902 (1988).
[15]S. G. Demos, L. Sheehan, and M. R. Kozlowski, in *Laser Applications in Microelectronic and Optoelectronic Applications V, Proc. SPIE* **3933**, 316 (2000).
[16]J. W. Chan, T. Huser, S. Risbud, and D. M. Krol, Optics Letters **26**, 1726 (2001).
[17]C. Meade, R. J. Hemley, and H. K. Mao, Phys. Rev. Lett. **69**, 1387 (1992).
[18]R. Couty and G. Sabatier, J. Chim. Phys. **75**, 843 (1978).
[19]L. V. Woodcock, C. A. Angel, and P. A. Cheeseman, J. Chem. Phys. **65**, 1565 (1976).
[20]W. Jin, R. K. Kalia, P. Vashishta, and J. P. Rino, Phys. Rev. Lett. **71**, 3146 (1993).
[21]D. J. Lacks, Phys. Rev. Lett. **84**, 4629 (2000).
[22]J. P. Rino, G. Gutierrez, I. Ebbsjo, R. K. Kalia, and P. Vashishta, Mat. Res. Soc. Symp. Proc. Vol. **408**, 333 (1996).
[23]P. S. Salmon, Nature **1**, 87 (2002).
[24]J. D. Martin, S. J. Goettler, N. Fosse, and L. Iton, Nature **419**, 381 (2002).
[25]E. B. Webb II and S. H. Garofalini, J. Chem. Phys. **101**, 10101 (1994).
[26]A. B. Belonoshko, Science, **275**, 955 (1997).
[27]A. Kubota, M.-J. Caturla, J. S. Stolken, and M. D. Feit, Opt. Express **8**, 611 (2001).
[28]Y. Inamura, M. Arai, M. Nakamura, T. Otomo, N. Kitamura, S. M. Bennington, A. C. Hannon, and U. Buchenau, J. Non-Cryst. Solids **293**, 389 (2001).
[29]S. R. Elliott, Nature **354**, 445 (1991); S. R. Elliott, Phys. Rev. B **51**, 8599 (1995).